

THE OSCILLATIONS OF RAPIDLY ROTATING NEWTONIAN STELLAR MODELS.  
II. DISSIPATIVE EFFECTS

JAMES R. IPSER

Department of Physics, University of Florida, Gainesville, FL 32611

AND

LEE LINDBLOM

Department of Physics, Montana State University, Bozeman, MT 59717

Received 1990 September 24; accepted 1990 October 30

## ABSTRACT

A method is described for determining the dissipative effects of viscosity and gravitational radiation on the modes of rapidly rotating Newtonian stellar models. Integral formulae for the dissipative imaginary parts of the frequencies (i.e., the damping or growth times) of these modes are derived. These expressions are evaluated numerically to determine the angular-velocity dependence of these dissipative effects on the  $l = m$   $f$ -modes of uniformly rotating polytropes. The importance of the gravitational-radiation driven secular instability in limiting the rotation rate of neutron stars is estimated using these results.

*Subject headings:* hydrodynamics — stars: neutron — stars: pulsation — stars: rotation

## 1. INTRODUCTION

This paper continues the study of the oscillations of rapidly rotating Newtonian stellar models that was begun by Iper & Lindblom (1989; 1990, hereafter referred to as Paper I). Paper I developed a method of finding the oscillation modes of rapidly rotating stars in terms of a single scalar potential  $\delta U$  for the case when the effects of dissipation could be neglected. In this paper we extend this analysis to include the dissipative effects of viscosity and gravitational radiation on these modes. The secular instabilities driven by these dissipative effects are widely believed to be the mechanism that limits the rotation rate of neutron stars (see, e.g., Friedman 1983; Wagoner 1984). Thus a careful analysis of these effects is essential in order to understand the range of this important observable quantity. The basic dissipative hydrodynamic equations are introduced in § 2 and equations for the dissipative imaginary parts of the frequencies of the oscillation modes are derived. In § 3 these dissipative time scales are evaluated numerically for sequences of rapidly rotating polytropes. Finally, in § 4, these dissipative time scales are used to compute the critical angular velocities above which rotating neutron stars are unstable.

## 2. EQUATIONS FOR THE DISSIPATIVE TIME SCALES

The state of a Newtonian fluid is specified by giving its mass density,  $\rho$ , and velocity,  $v^a$ , at each point. The equations that describe the evolution of these quantities, including the effects of viscosity and gravitational-radiation reaction, are (see for example Landau & Lifshitz 1975)

$$\partial_t \rho + \nabla_a (\rho v^a) = 0, \quad (1)$$

and

$$\partial_t v^a + v^b \nabla_b v^a + \nabla^a U = \nabla^a \Phi_{\text{GR}} + 2\rho^{-1} \nabla_b (\eta \sigma^{ab}) + \rho^{-1} \nabla^a (\zeta \sigma). \quad (2)$$

In these equations  $\partial_t$  and  $\nabla_a$  represent the partial derivative with respect to time,  $t$ , and the spatial Euclidean covariant-derivative (i.e., just the partial derivatives  $\partial/\partial x^a$  in Cartesian coordinates) respectively. The potential  $U$  is defined as

$U = h - \Phi$ , where  $h$  is given by the integral

$$h(p) = \int_0^p \frac{dp'}{\rho(p')}, \quad (3)$$

and  $p$  is the pressure of the fluid. The Newtonian gravitational potential,  $\Phi$ , satisfies the equation

$$\nabla^a \nabla_a \Phi = -4\pi G \rho, \quad (4)$$

where  $G$  is the gravitational constant. The potential  $\Phi_{\text{GR}}$  couples the fluid to gravitational-radiation reaction (see, e.g., Thorne 1969) by the formula

$$\Phi_{\text{GR}} = - \sum_{l=2}^{\infty} \sum_{m=-l}^l (-1)^l N_l r^l Y_l^m \frac{d^{2l+1} D_l^m}{dt^{2l+1}}, \quad (5)$$

where  $D_l^m$  is the mass multipole,

$$D_l^m = \int \rho r^l Y_l^{*m} d^3x, \quad (6)$$

$$N_l = \frac{4\pi G}{c^{2l+1}} \frac{(l+1)(l+2)}{l(l-1)[(2l+1)!]^2}, \quad (7)$$

and  $c$  is the speed of light. Finally,  $\eta$  and  $\zeta$  are the shear- and bulk-viscosity coefficients (which are taken to be given functions of  $\rho$ ), while  $\sigma^{ab}$  and  $\sigma$  are the shear and the expansion, given by

$$\sigma^{ab} = \frac{1}{2}(\nabla^a v^b + \nabla^b v^a - \frac{2}{3}g^{ab}\nabla_c v^c), \quad (8)$$

and

$$\sigma = \nabla_a v^a. \quad (9)$$

The tensor  $g_{ab}$ , the Euclidean metric (i.e., the identity matrix in Cartesian coordinates), and its inverse,  $g^{ab}$ , are used to raise and lower tensor indices.

The time-independent (i.e., equilibrium) solutions of these equations are the rigidly rotating subset of those considered in Paper I. In particular the fluid velocity,  $v^a = \Omega \phi^a = \omega^2 \Omega \nabla^a \phi$ , is a constant multiple of  $\phi^a$  which satisfies Killing's equation,  $0 = \nabla_a \phi_b + \nabla_b \phi_a$ ; i.e.,

$$\nabla_a \Omega = 0. \quad (10)$$

Throughout this paper we refer to the standard spherical coordinates as  $r$ ,  $\theta$ , and  $\phi$ , and the cylindrical radial coordinate as  $\varpi = r \sin \theta$ . The fluid equation (2), can be integrated completely under these circumstances, with the result

$$C = h(p) - \Phi - \frac{1}{2}\varpi^2\Omega^2, \quad (11)$$

where  $C$  is a constant, and  $\Phi$  satisfies equation (4). The procedure that we use to find numerical solutions to these equations, representing models of rotating stars, is described in Paper I.

We now consider the equations for the evolution of small perturbations of an equilibrium solution. We denote the (Eulerian) perturbation of a quantity  $q$  by  $\delta q$ . In the equations that follow, any function not prefaced by  $\delta$  is assumed to be evaluated in the equilibrium solution. We begin by linearizing equations (1)–(4) about an arbitrary equilibrium solution. The resulting equations are given by

$$\partial_t \delta \rho + v^a \nabla_a \delta \rho + \nabla_a (\rho \delta v^a) = 0, \quad (12)$$

$$\begin{aligned} \partial_t \delta v^a + v^b \nabla_b \delta v^a + \delta v^b \nabla_b v^a + \nabla^a \delta U \\ = \nabla^a \delta \Phi_{\text{GR}} + 2\rho^{-1} \nabla_b (\eta \delta \sigma^{ab}) + \rho^{-1} \nabla^a (\zeta \delta \sigma), \end{aligned} \quad (13)$$

and

$$\nabla^a \nabla_a \delta \Phi = -4\pi G \delta \rho. \quad (14)$$

Next, we introduce an “energy” of the perturbations:

$$E(t) = \frac{1}{2} \int \left[ \rho \delta v^a \delta v_a^* + \frac{1}{2} (\delta \rho \delta U^* + \delta \rho^* \delta U) \right] d^3x, \quad (15)$$

where  $*$  represents complex conjugation and  $\delta U = \delta p/\rho - \delta \Phi$ . The time derivative of this quantity can be evaluated using equations (12)–(14), with the result

$$\begin{aligned} \frac{dE}{dt} = - \int (2\eta \delta \sigma^{ab} \delta \sigma_{ab}^* + \zeta \delta \sigma \delta \sigma^*) d^3x \\ - \frac{1}{2} \sum_{l=2}^{\infty} \sum_{m=-l}^l (-1)^l N_l \left[ \frac{d^{2l+1} \delta D_l^m}{dt^{2l+1}} \left( \frac{d \delta D_l^{*m}}{dt} - im\Omega \delta D_l^{*m} \right) \right. \\ \left. + \frac{d^{2l+1} \delta D_l^{*m}}{dt^{2l+1}} \left( \frac{d \delta D_l^m}{dt} + im\Omega \delta D_l^m \right) \right]. \end{aligned} \quad (16)$$

In this expression the perturbed quantities  $\delta \sigma^{ab}$ ,  $\delta \sigma$ , and  $\delta D_l^m$  are related to the perturbations of the fundamental fluid variables  $\delta \rho$  and  $\delta v^a$  by

$$\delta \sigma^{ab} = \frac{1}{2} (\nabla^a \delta v^b + \nabla^b \delta v^a - \frac{2}{3} g^{ab} \nabla_c \delta v^c), \quad (17)$$

$$\delta \sigma = \nabla_a \delta v^a, \quad (18)$$

and

$$\delta D_l^m = \int \delta r^l Y_l^{*m} d^3x. \quad (19)$$

We now assume that all perturbed quantities have sinusoidal dependence in the coordinates  $t$  and  $\varphi$ :  $\delta q = \delta q(r, \theta) e^{i\omega t + im\varphi}$ , where  $\omega$  is the frequency of the mode and  $m$  is an integer. Under this assumption, the time derivative of the energy,  $E$ , is related to the imaginary part of the frequency,  $1/\tau \equiv \text{Im}(\omega)$ , as follows

$$\frac{dE}{dt} = - \frac{2E}{\tau}. \quad (20)$$

We can use this equation to obtain explicit integral formulae

for the contributions to the imaginary part of the frequency from each of the dissipative mechanisms:

$$\frac{1}{\tau_\zeta} = \frac{1}{2E} \int \zeta \delta \sigma \delta \sigma^* d^3x, \quad (21)$$

$$\frac{1}{\tau_\eta} = \frac{1}{E} \int \eta \delta \sigma^{ab} \delta \sigma_{ab}^* d^3x, \quad (22)$$

and

$$\frac{1}{\tau_{\text{GR}}} = \frac{\omega + m\Omega}{2E} \sum_{l=l_{\text{min}}}^{\infty} N_l \omega^{2l+1} \delta D_l^m \delta D_l^{*m}, \quad (23)$$

where  $l_{\text{min}}$  is the larger of 2 or  $|m|$ . The imaginary part of the frequency is the sum of these individual contributions:  $1/\tau = 1/\tau_\zeta + 1/\tau_\eta + 1/\tau_{\text{GR}}$ .

The expressions, equations (21)–(23), for the damping times  $\tau_\zeta$ ,  $\tau_\eta$ , and  $\tau_{\text{GR}}$  are identities that are satisfied by the solutions to equations (12)–(14). Since these equations are not easily solved, the expressions, equations (21)–(23), are not directly useful. However, when the effects of dissipation are small (i.e., when  $\zeta$ ,  $\eta$ , and  $N_l$  are small in a suitable sense) these expressions can be used to obtain useful approximations for  $\tau_\zeta$ ,  $\tau_\eta$ ,  $\tau_{\text{GR}}$ . Under these circumstances, the exact solutions to the perturbation equations for  $\delta \rho$ ,  $\delta v^a$ , and  $\omega$  are nearly identical to the corresponding solutions to the nondissipative perturbation equations. In this case  $\delta \rho$  and  $\delta v^a$  are determined (approximately) by the single potential  $\delta U$ :

$$\delta \rho = - \frac{\nabla_a (\rho Q^{ab} \nabla_b \delta U)}{\omega + m\Omega}, \quad (24)$$

$$\delta v^a = iQ^{ab} \nabla_b \delta U, \quad (25)$$

as described in Paper I. In these equations,  $\omega$  represents the real frequency of the nondissipative pulsations, and  $Q^{ab}$  is given by

$$Q^{ab} = \frac{1}{\omega + m\Omega} \left[ \lambda g^{ab} + (1 - \lambda) z^a z^b - \frac{2i\lambda \Omega \nabla^a \phi^b}{\omega + m\Omega} \right], \quad (26)$$

where  $\lambda = (\omega + m\Omega)^2 / [(\omega + m\Omega)^2 - 4\Omega^2]$ . (We note that  $Q^{ab} = Q^{*ba}$  and  $\nabla_c Q^{ab} = 0$ .) Using equations (24) and (25), the damping times  $\tau_\zeta$  and  $\tau_\eta$  may then be expressed (approximately) as the following integrals involving the derivatives of  $\delta U$ :

$$E = \frac{1}{2} \int \rho \nabla_a \delta U^* \left[ Q_c^a Q^{cb} + \frac{Q^{ab}}{\omega + m\Omega} \right] \nabla_b \delta U d^3x, \quad (27)$$

$$\frac{1}{\tau_\zeta} = \frac{1}{2E} \int \zeta \nabla_a \nabla_b \delta U^* Q^{ab} Q^{cd} \nabla_c \nabla_d \delta U d^3x, \quad (28)$$

and

$$\begin{aligned} \frac{1}{\tau_\eta} = \frac{1}{2E} \int \eta \nabla_a \nabla_b \delta U^* \\ \times \left( Q_e^a Q^{ec} g^{bd} + Q^{ac} Q^{bd} - \frac{2}{3} Q^{ab} Q^{cd} \right) \nabla_c \nabla_d \delta U d^3x. \end{aligned} \quad (29)$$

The gravitational-radiation damping time,  $\tau_{\text{GR}}$ , is approximated from equation (23) by using for  $\omega$  the nondissipative value of the frequency, and for  $\delta D_l^m$ ,

$$\delta D_l^m = - \frac{1}{\omega + m\Omega} \int r^l Y_l^{*m} \nabla_a (\rho Q^{ab} \nabla_b \delta U) d^3x. \quad (30)$$

TABLE 1  
PHYSICAL PARAMETERS OF NONROTATING POLYTOPES

$n^a$	$\frac{M}{M_\odot}$	$R$ (km)	$\frac{\bar{\rho}_0}{10^{14}}$ ( $\text{g cm}^{-3}$ )	$\Omega_0$ ( $\text{s}^{-1}$ ) <sup>b</sup>	$T$ (K)
0	1.0	15.000	1.407	5431	$10^9$
	1.5	17.171	1.407	5431	$10^9$
	2.0	18.899	1.407	5431	$10^9$
3/4	1.0	13.617	1.881	6279	$10^9$
	1.5	14.245	2.464	7188	$10^9$
	2.0	14.707	2.985	7911	$10^9$
1	1.0	12.533	2.412	7111	$10^9$
	1.5	12.533	3.618	8709	$10^9$
	2.0	12.533	4.824	10056	$10^9$
5/4	1.0	10.407	4.213	9397	$10^9$
	1.5	9.822	7.517	12554	$10^9$
	2.0	9.426	11.339	15416	$10^9$

<sup>a</sup> Index  $n$  is the parameter in the polytropic equation of state:  $p = \kappa \rho^{1+1/n}$ .

<sup>b</sup> Frequencies and damping times are given in units of  $\Omega_0 = (\pi G \bar{\rho}_0)^{1/2}$ , where  $\bar{\rho}_0$  is the average density of the nonrotating star.

These expressions provide first approximations for the values of the dissipative damping times  $\tau_\zeta$ ,  $\tau_\eta$ , and  $\tau_{\text{GR}}$ . In neutron stars the effects of dissipation are in fact suitably small, since the pulsation periods are much shorter than the damping times, i.e.,  $\omega\tau \gg 1$  (see Table 2). Thus, these expressions are excellent approximations of the imaginary parts of the frequency.

### 3. DISSIPATIVE TIME SCALES OF ROTATING POLYTOPES

The dissipative time scales  $\tau_\zeta$ ,  $\tau_\eta$ , and  $\tau_{\text{GR}}$  have been evaluated numerically for the  $l = m$   $f$ -modes of a range of uniformly rotating polytropic stellar models. The parameters in the polytropic equations of state were selected so that the macroscopic

properties of these models approximate those of more realistic neutron-star models. The index  $n$  in the polytropic equation of state,  $p = \kappa \rho^{1+1/n}$ , was chosen to ensure that the central condensations of these models were comparable to those of more realistic neutron stars. The values  $n = 3/4, 1,$  and  $5/4$  roughly span the range of realistic equations of state that have been proposed (see, e.g., Cutler, Lindblom, & Splinter 1990). The parameter  $\kappa$  in each equation of state was chosen so that the radius of the  $1.5 M_\odot$  stellar model is comparable to a model having comparable central condensation based on a more realistic equation of state. In cgs units the chosen values are  $\kappa = 1.3346, 6.637 \times 10^4,$  and  $4.0038 \times 10^7$  for the  $n = 3/4, 1,$  and  $5/4$  polytropes, respectively. Since analytic formulae exist to describe the structure, pulsations, and damping of the  $n = 0$  polytropes (the Maclaurin spheroids, see Lindblom 1986), these models have been included in this study for comparison purposes. Table 1 summarizes the macroscopic parameters of the nonrotating Newtonian stellar models used in this study. Sequences of uniformly rotating stellar models having the same total mass as these nonrotating models were also constructed. The numerical method used to construct these stellar models is described in Paper I.

In order to evaluate the dissipative time scales, expressions for the viscosities appropriate for neutron-star matter are needed. The bulk viscosity  $\zeta$  arises as a result of the phase lag that occurs between density and pressure perturbations in neutron-star matter due to the relatively long time scale required for the weak interactions to re-establish equilibrium. For normal nuclear matter, Sawyer (1989) finds this bulk viscosity to be given by

$$\zeta = 6.0 \times 10^{25} \left( \frac{\rho_{15}}{\omega} \right)^2 T_9^6, \quad (31)$$

where  $\zeta$  has units  $\text{g cm}^{-1} \text{s}^{-1}$ ,  $\rho_{15}$  has units  $10^{15} \text{ g cm}^{-3}$ ,  $T_9$

TABLE 2  
DAMPING TIMES AND PULSATION FREQUENCIES FOR  $1.5 M_\odot$  NONROTATING POLYTOPES

$l = m$	$n^a$	$\frac{\omega(0)^b}{\Omega_0}$	$\tau_{\text{GR}} \Omega_0$	$\tau_{\eta} \Omega_0$	$\tau_{\nu} \Omega_0$	$\tau_\zeta \Omega_0$
2	0	1.033	$2.84 \times 10^3$	$1.07 \times 10^{13}$	$3.80 \times 10^{12}$	...
	3/4	1.292	$5.44 \times 10^2$	$1.97 \times 10^{12}$	$5.60 \times 10^{11}$	$1.70 \times 10^{18}$
	1	1.415	$2.43 \times 10^2$	$6.00 \times 10^{11}$	$2.05 \times 10^{11}$	$1.85 \times 10^{17}$
	5/4	1.543	$8.46 \times 10^1$	$1.09 \times 10^{11}$	$4.95 \times 10^{10}$	$3.29 \times 10^{16}$
3	0	1.512	$1.65 \times 10^5$	$3.81 \times 10^{12}$	$1.36 \times 10^{12}$	...
	3/4	1.819	$2.55 \times 10^4$	$1.57 \times 10^{12}$	$3.94 \times 10^{11}$	$2.13 \times 10^{18}$
	1	1.959	$1.06 \times 10^4$	$6.15 \times 10^{11}$	$1.80 \times 10^{11}$	$2.66 \times 10^{17}$
	5/4	2.095	$3.11 \times 10^3$	$1.47 \times 10^{11}$	$5.54 \times 10^{10}$	$5.57 \times 10^{16}$
4	0	1.886	$1.03 \times 10^7$	$1.98 \times 10^{12}$	$7.04 \times 10^{11}$	...
	3/4	2.208	$1.34 \times 10^6$	$1.47 \times 10^{12}$	$3.34 \times 10^{11}$	$3.48 \times 10^{18}$
	1	2.350	$5.21 \times 10^5$	$7.00 \times 10^{11}$	$1.81 \times 10^{11}$	$4.90 \times 10^{17}$
	5/4	2.481	$1.30 \times 10^5$	$2.08 \times 10^{11}$	$6.69 \times 10^{10}$	$1.19 \times 10^{17}$
5	0	2.202	$7.35 \times 10^8$	$1.21 \times 10^{12}$	$4.32 \times 10^{11}$	...
	3/4	2.526	$8.17 \times 10^7$	$1.42 \times 10^{12}$	$3.02 \times 10^{11}$	$5.90 \times 10^{18}$
	1	2.667	$2.95 \times 10^7$	$7.98 \times 10^{11}$	$1.87 \times 10^{11}$	$9.14 \times 10^{17}$
	5/4	2.789	$6.21 \times 10^6$	$2.81 \times 10^{11}$	$7.94 \times 10^{10}$	$2.52 \times 10^{17}$
6	0	2.481	$5.94 \times 10^{10}$	$8.23 \times 10^{11}$	$2.92 \times 10^{11}$	...
	3/4	2.812	$5.84 \times 10^9$	$1.39 \times 10^{12}$	$2.80 \times 10^{11}$	$9.83 \times 10^{18}$
	1	2.939	$1.92 \times 10^9$	$8.99 \times 10^{11}$	$1.93 \times 10^{11}$	$1.65 \times 10^{18}$
	5/4	3.053	$3.39 \times 10^8$	$3.63 \times 10^{11}$	$9.20 \times 10^{10}$	$5.07 \times 10^{17}$

<sup>a</sup> Index  $n$  is the parameter in the polytropic equation of state:  $p = \kappa \rho^{1+1/n}$ .

<sup>b</sup> Frequencies and damping times are given in units of  $\Omega_0 = (\pi G \bar{\rho}_0)^{1/2}$ , where  $\bar{\rho}_0$  is the average density of the nonrotating star.

has units  $10^9$  K, and  $\omega$  has units  $s^{-1}$ . The shear viscosity  $\eta$  arises as the result of momentum transport within the fluid due to the scattering of particles. For neutron-star matter hotter than the superfluid transition temperature ( $T \gtrsim 10^9$  K) this scattering is dominated by neutron-neutron interactions. The resulting viscosity  $\eta_n$  has been calculated by Flowers & Itoh (1976). The following analytical fit reproduces their result to within a few percent:

$$\eta_n = 1.95 \times 10^{18} \frac{\rho_{15}^{9/4}}{T_9^2}, \quad (32)$$

where  $\eta_n$  has units  $g \text{ cm}^{-1} \text{ s}^{-1}$ . For neutron stars cooler than the superfluid-transition temperature the viscosity is thought to be dominated by electron-electron scattering. The expression

$$\eta_e = 6.0 \times 10^{18} \left( \frac{\rho_{15}}{T_9} \right)^2, \quad (33)$$

reproduces the exact electron-electron scattering result to within a few percent at neutron star densities (Cutler & Lindblom 1987).

The time scales  $\tau_\zeta$ ,  $\tau_\eta$ , and  $\tau_{GR}$  are evaluated using equations (21), (22), and (23). In these expressions the quantities  $E$ ,  $\delta\sigma$ ,  $\delta\sigma^{ab}$ , and  $\delta D_l^m$  are evaluated in terms of the potential  $\delta U$  as described in equations (24)–(30). This potential is the solution of the nondissipative pulsation equations, and is evaluated by the procedure described in Paper I. Thus, the problem of finding the dissipative time scales is reduced to the evaluation of the quadratures in equations (27)–(30). It is straightforward to evaluate these integrals using the expressions for the viscosity coefficients in equations (31)–(33).

Figures 1–3 illustrate the integrands in equations (19), (21), and (22), respectively, for the  $l = m = 4$   $f$ -mode of the  $1.5 M_\odot$  polytrope of index  $n = 1$  rotating with angular velocity  $\Omega = 0.6\Omega_0$ , where  $\Omega_0 = (\pi G \bar{\rho}_0)^{1/2}$  and  $\bar{\rho}_0$  is the average density of the nonrotating star of the same mass. Each curve in these figures represents the  $r$ -dependence of the particular integrand along one of the 10 angular spokes used to compute this model. For these figures the normalization was chosen so that the maximum value of each integrand was one. These integrands were derived from the  $\delta U(r, \mu_i)$  depicted in Figure 9 of

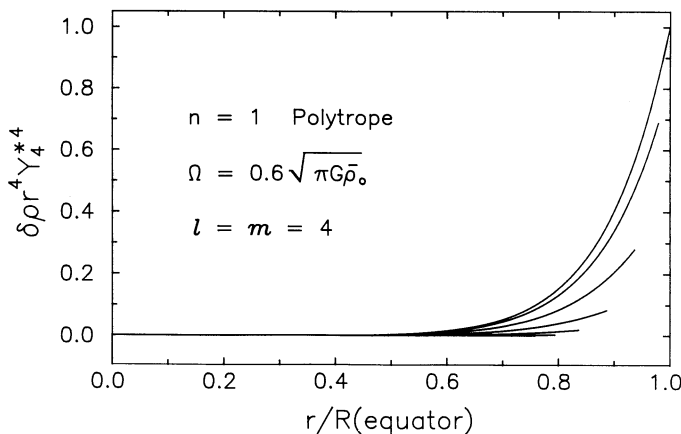


FIG. 1.—Integrand that determines the gravitational-radiation time scale for the  $l = m = 4$  mode of the  $1.5 M_\odot$  polytrope of index  $n = 1$  which rotates with angular velocity  $\Omega = 0.6(\pi G \bar{\rho}_0)^{1/2}$ , where  $\bar{\rho}_0$  is the average density of the nonrotating star of the same mass.

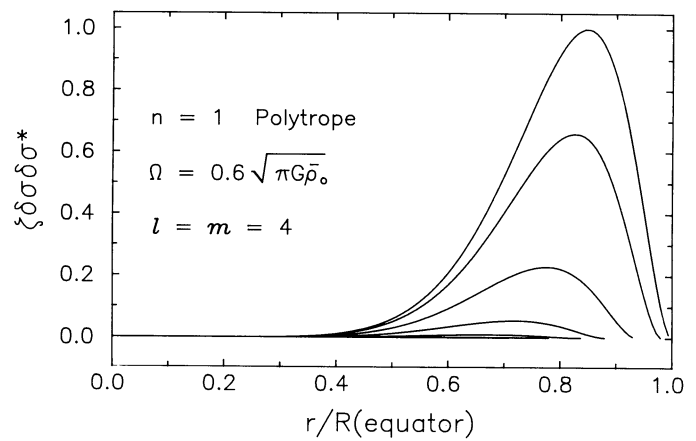


FIG. 2.—Integrand that determines the bulk-viscosity time-scale for the  $l = m = 4$  mode of the  $1.5 M_\odot$  polytrope of index  $n = 1$  which rotates with angular velocity  $\Omega = 0.6(\pi G \bar{\rho}_0)^{1/2}$ , where  $\bar{\rho}_0$  is the average density of the nonrotating star of the same mass.

Paper I. The integrand that determines the gravitational-radiation reaction, Figure 1, is very strongly peaked on the equator and at the surface of the star. The bulk viscosity, Figure 2, and the shear viscosity, Figure 3, integrands are successively less strongly peaked. The fluid densities where the functions in Figures 2 and 3 achieve their maxima are in the range  $1 \sim 3 \times 10^{14} \text{ g cm}^{-3}$ . Thus the use of the viscosity formulae, equations (31)–(33), appropriate for the nuclear density regime is justified.

Table 2 summarizes the values of the oscillation frequencies and the dissipative time scales for the  $2 \leq l = m \leq 6$   $f$ -modes of the  $1.5 M_\odot$  nonrotating stellar models described in Table 1. These frequencies and time scales have simple scaling laws in terms of the mass  $M$ , radius  $R$ , and temperature  $T$  for these polytropic stellar models. The quantity  $\omega/\Omega_0$  depends only on the polytropic index  $n$ , not on  $M$ ,  $R$ , or  $T$ ;  $\tau_{GR} \Omega_0$  scales as  $(R/M)^{(2l+1)/2}$ ;  $\tau_{\eta_n} \Omega_0$  scales as  $R^{17/4} T^2 / M^{3/4}$ ;  $\tau_{\eta_e} \Omega_0$  scales as  $R^{7/2} T^2 / M^{1/2}$ ; and  $\tau_\zeta \Omega_0$  scales as  $M^{1/2} R^{1/2} / T^6$ . For a given polytropic index  $n$ , these quantities depend on the parameter  $\kappa$  (in the polytropic equation of state) and the central density of the star only through these scalings. As one check of our com-

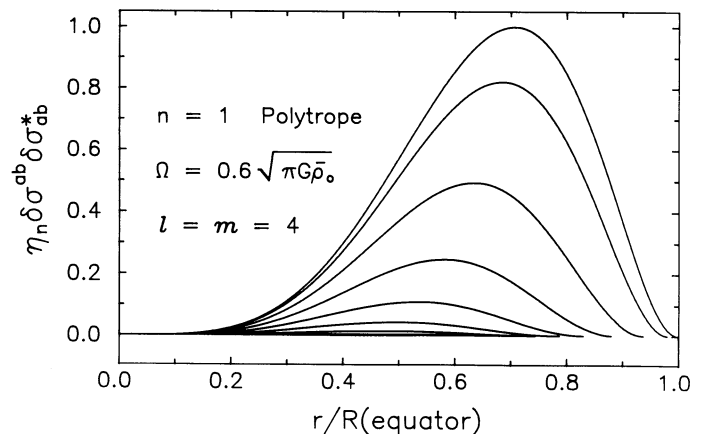


FIG. 3.—Integrand that determines the shear-viscosity time scale for the  $l = m = 4$  mode of the  $1.5 M_\odot$  polytrope of index  $n = 1$  which rotates with angular velocity  $\Omega = 0.6(\pi G \bar{\rho}_0)^{1/2}$ , where  $\bar{\rho}_0$  is the average density of the nonrotating star of the same mass.

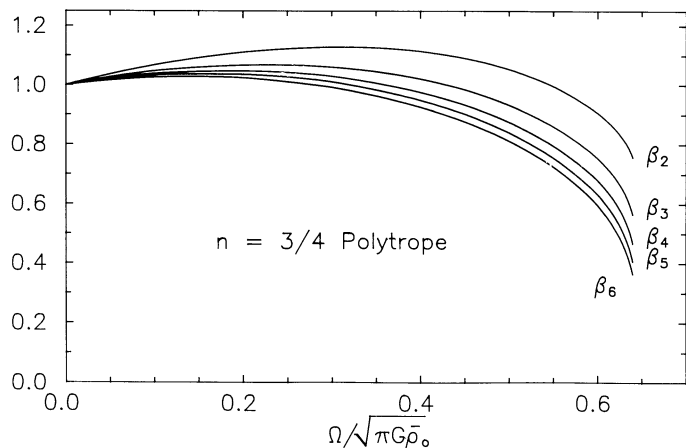


FIG. 4.—Functions  $\beta_m(\Omega)$  of the angular velocity for the  $l = m$   $f$ -modes of  $n = 3/4$  polytropes. The angular velocities are given in units of  $(\pi G \bar{\rho}_0)^{1/2}$ , where  $\bar{\rho}_0$  is the average density of the nonrotating star of the same mass.

puter code, we have verified that the numerically determined values of these quantities do scale in the appropriate ways.

It is convenient to describe the angular velocity dependence of the dissipative time scales  $\tau_\eta$ ,  $\tau_{GR}$ ,  $\tau_\zeta$  in terms of dimensionless functions  $\beta(\Omega)$ ,  $\gamma(\Omega)$ , and  $\epsilon(\Omega)$ . These functions are defined by the expressions

$$\beta(\Omega) = \frac{\tau_\eta(0)}{\tau_\eta(\Omega)}, \quad (34)$$

$$\gamma(\Omega) = \frac{\omega(\Omega)}{\omega(0)} \left[ \frac{\tau_\eta(0)}{\tau_{GR}(0)} \frac{\tau_{GR}(\Omega)}{\tau_\eta(\Omega)} \right]^{1/(2l+1)}, \quad (35)$$

$$\epsilon(\Omega) = \frac{\tau_\zeta(0)}{\tau_\eta(0)} \frac{\tau_\eta(\Omega)}{\tau_\zeta(\Omega)} \left[ 1 - \left( \frac{\Omega}{\Omega_{\max}} \right)^4 \right], \quad (36)$$

where  $\Omega_{\max}$  is the angular velocity where the sequence of equilibrium models terminates. The functions  $\beta_m(\Omega)$  for the  $l = m$   $f$ -modes are illustrated in Figures 4–7. Figures 4–6 illustrate the dependence of  $\beta_m$  on the mode number for the  $n = 3/4$ , 1, and  $5/4$  polytropes, respectively. Figure 7 illustrates more directly the dependence of these functions on the equation of state, for the single mode  $l = m = 4$ . Similarly Figures 8–11 illustrate

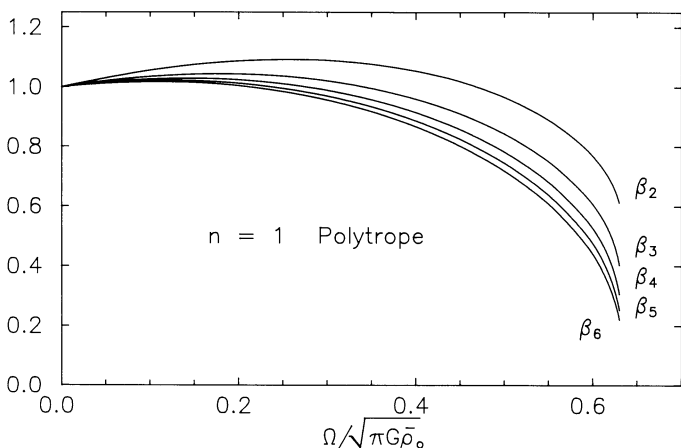


FIG. 5.—Functions  $\beta_m(\Omega)$  of the angular velocity for the  $l = m$   $f$ -modes of  $n = 1$  polytropes. The angular velocities are given in units of  $(\pi G \bar{\rho}_0)^{1/2}$ , where  $\bar{\rho}_0$  is the average density of the nonrotating star of the same mass.

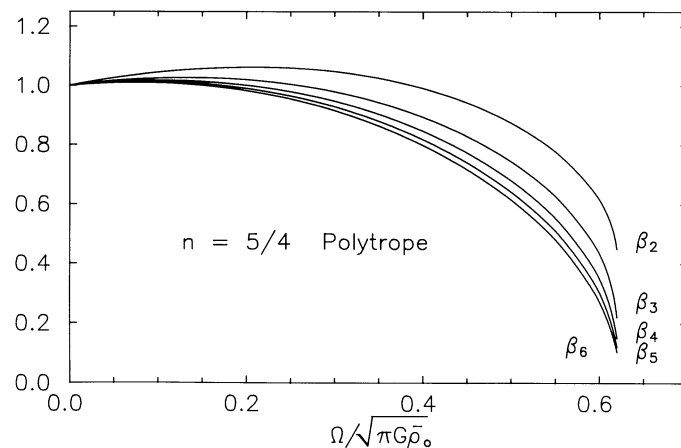


FIG. 6.—Functions  $\beta_m(\Omega)$  of the angular velocity for the  $l = m$   $f$ -modes of  $n = 5/4$  polytropes. The angular velocities are given in units of  $(\pi G \bar{\rho}_0)^{1/2}$ , where  $\bar{\rho}_0$  is the average density of the nonrotating star of the same mass.

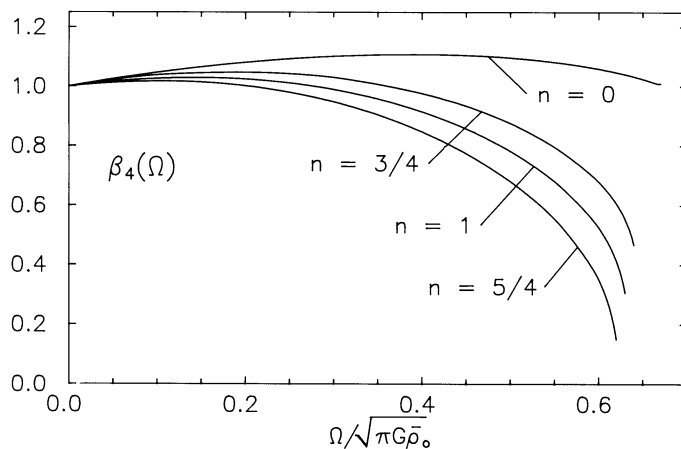


FIG. 7.—Functions  $\beta_4(\Omega)$  of the angular velocity for the  $l = m = 4$   $f$ -modes of rotating  $n = 0, 3/4, 1,$  and  $5/4$  polytropes. The angular velocities are given in units of  $(\pi G \bar{\rho}_0)^{1/2}$ , where  $\bar{\rho}_0$  is the average density of the nonrotating star of the same mass.

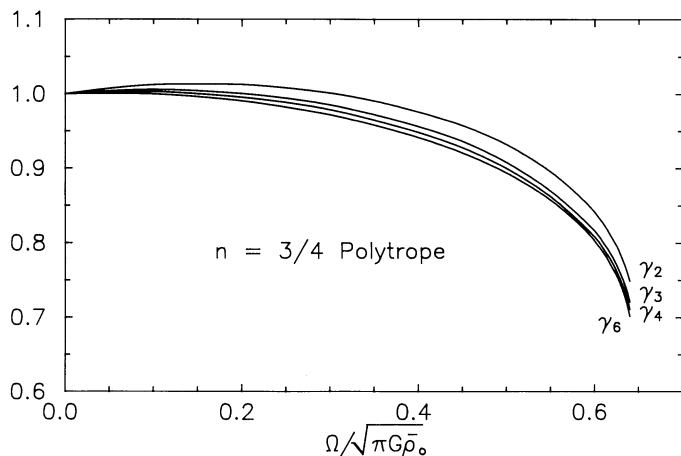


FIG. 8.—Functions  $\gamma_m(\Omega)$  of the angular velocity for the  $l = m$   $f$ -modes of  $n = 3/4$  polytropes. The angular velocities are given in units of  $(\pi G \bar{\rho}_0)^{1/2}$ , where  $\bar{\rho}_0$  is the average density of the non-rotating star of the mass.



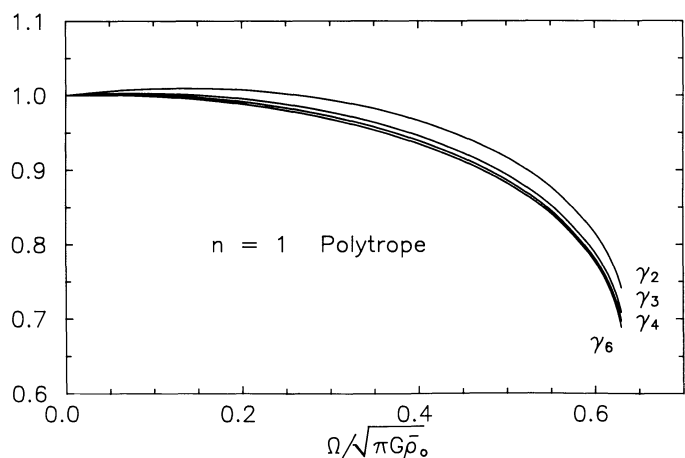


FIG. 9.—Functions  $\gamma_m(\Omega)$  of the angular velocity for the  $l = m$   $f$ -modes of  $n = 1$  polytropes. The angular velocities are given in units of  $(\pi G \bar{\rho}_0)^{1/2}$ , where  $\bar{\rho}_0$  is the average density of the nonrotating star of the same mass.

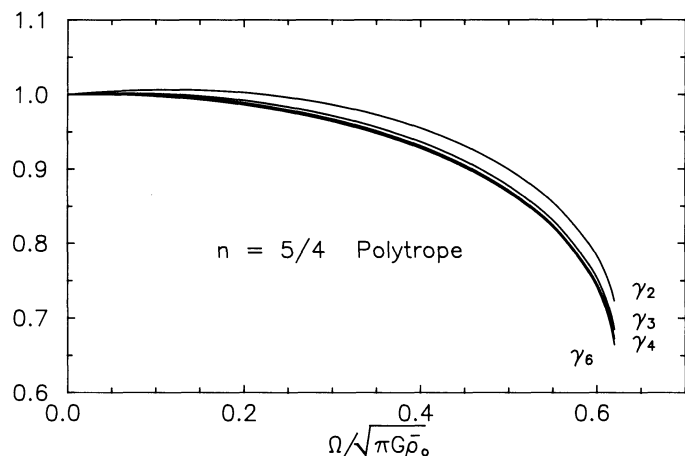


FIG. 10.—Functions  $\gamma_m(\Omega)$  of the angular velocity for the  $l = m$   $f$ -modes of  $n = 5/4$  polytropes. The angular velocities are given in units of  $(\pi G \bar{\rho}_0)^{1/2}$ , where  $\bar{\rho}_0$  is the average density of the nonrotating star of the same mass.

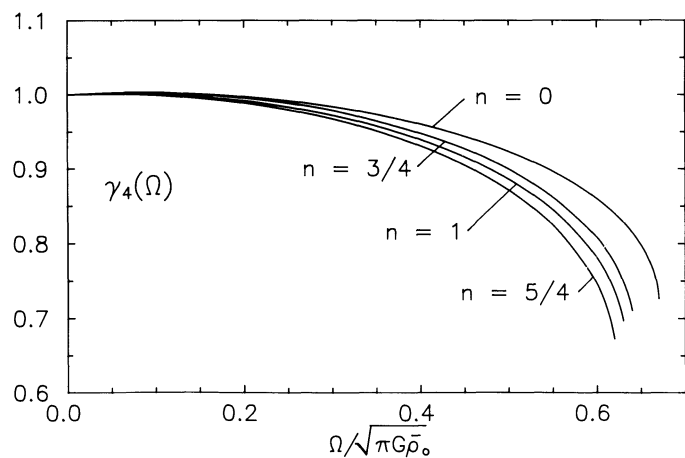


FIG. 11.—Functions  $\gamma_4(\Omega)$  of the angular velocity for the  $l = m = 4$   $f$ -modes of rotating  $n = 0, 3/4, 1,$  and  $5/4$  polytropes. The angular velocities are given in units of  $(\pi G \bar{\rho}_0)^{1/2}$ , where  $\bar{\rho}_0$  is the average density of the nonrotating star of the same mass.

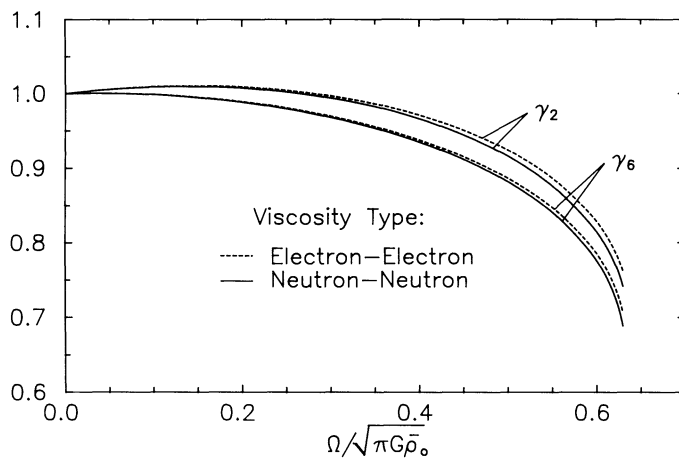


FIG. 12.—Functions  $\gamma_m(\Omega)$  of the angular velocity for two choices of the shear viscosity: neutron-neutron scattering viscosity  $\eta_n$  and electron-electron scattering viscosity  $\eta_e$ . The angular velocities are given in units of  $(\pi G \bar{\rho}_0)^{1/2}$ , where  $\bar{\rho}_0$  is the average density of the nonrotating star of the same mass.

the dependence of the functions  $\zeta_m(\Omega)$  on the mode number and the equation of state. Figure 12 illustrates the dependence of  $\gamma_m(\Omega)$  on the expression used for the shear viscosity. And finally, Figures 13–16 illustrate the dependence of the functions  $\epsilon_m(\Omega)$  on the mode number and the equation of state. These functions do not depend on the equation of state other than through their dependence on the polytropic index  $n$ . These functions do not depend on the mass of the star. Note that these are all fairly slowly varying functions of angular velocity. The “extraneous” angular velocity dependence  $1 - (\Omega/\Omega_{\max})^4$  was introduced empirically into the definition of  $\epsilon_m(\Omega)$ , equation (36), in order that it be a slowly varying function. This was necessary because the bulk-viscous time scale  $\tau_\zeta$  becomes much shorter in rapidly rotating stars than it is in the nonrotating models of the same mass.

#### 4. CRITICAL ANGULAR VELOCITIES OF ROTATING POLYTOPES

The oscillations of a rotating star will be stable as long as the imaginary part of the frequency  $1/\tau$  of that mode is positive. The viscous contributions  $1/\tau_\zeta$  and  $1/\tau_\eta$  are positive as a consequence of equations (21) and (22). In contrast, the

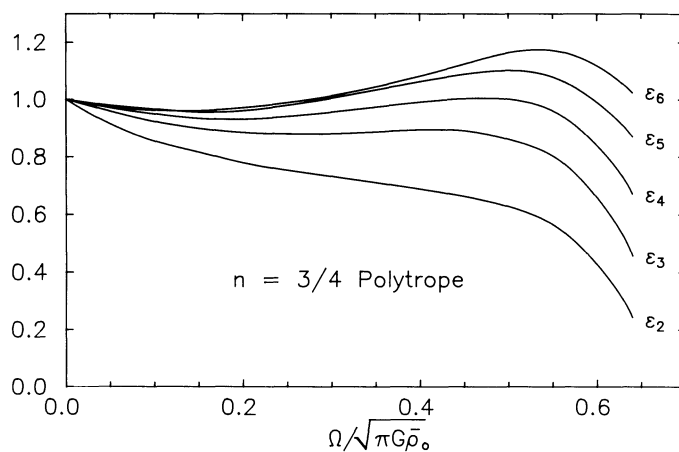


FIG. 13.—Functions  $\epsilon_m(\Omega)$  of the angular velocity of the  $l = m$   $f$ -modes of  $n = 3/4$  polytropes. The angular velocities are given in units of  $(\pi G \bar{\rho}_0)^{1/2}$ , where  $\bar{\rho}_0$  is the average density of the nonrotating star of the same mass.

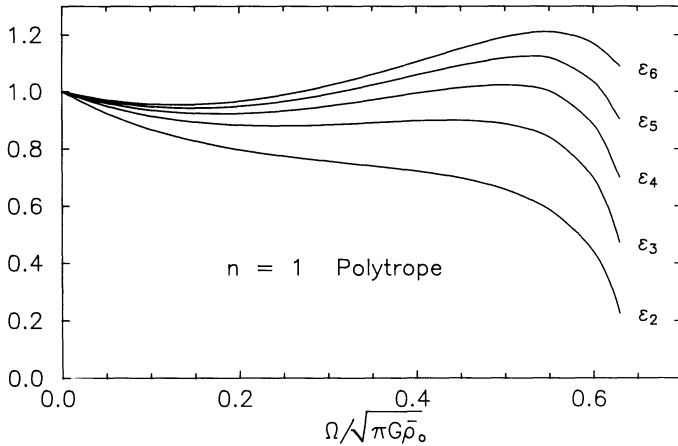


FIG. 14.—Functions  $\epsilon_m(\Omega)$  of the angular velocity for the  $l = m$   $f$ -modes of  $n = 1$  polytropes. The angular velocities are given in units of  $(\pi G \bar{\rho}_0)^{1/2}$ , where  $\bar{\rho}_0$  is the average density of the nonrotating star of the same mass.

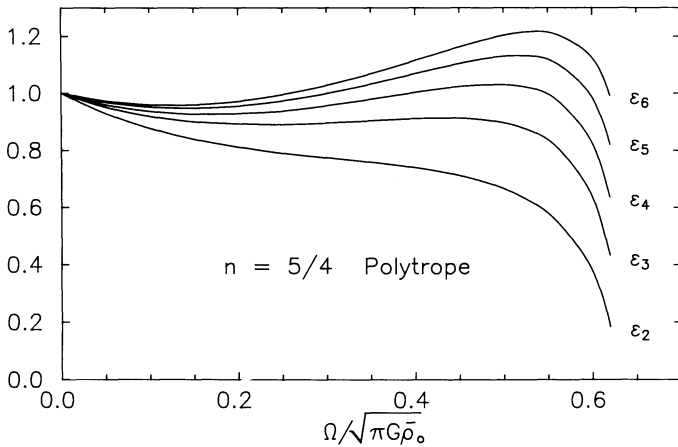


FIG. 15.—Functions  $\epsilon_m(\Omega)$  of the angular velocity for the  $l = m$   $f$ -modes of  $n = 5/4$  polytropes. The angular velocities are given in units of  $(\pi G \bar{\rho}_0)^{1/2}$ , where  $\bar{\rho}_0$  is the average density of the nonrotating star of the same mass.

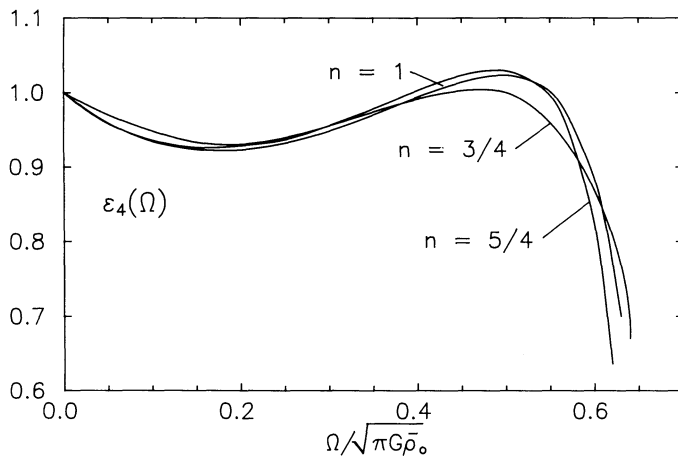


FIG. 16.—Functions  $\epsilon_4(\Omega)$  of the angular velocity for the  $l = m = 4$   $f$ -modes of rotating  $n = 0, 3/4, 1,$  and  $5/4$  polytropes. The angular velocities are given in units of  $(\pi G \bar{\rho}_0)^{1/2}$ , where  $\bar{\rho}_0$  is the average density of the nonrotating star of the same mass.

gravitational-radiation contribution  $1/\tau_{\text{GR}}$  is proportional to  $\omega^{2l+1}$ , equation (23), and so changes sign whenever  $\omega$  changes sign. Thus, an instability will occur in a rotating star whenever  $\omega$  is sufficiently negative. For the  $l = m$  modes considered in this paper,  $\omega_m$  is positive for nonrotating stars and decreases monotonically as the angular velocity of the star is increased. Thus, these modes are stable in slowly rotating stars, while for sufficiently rapidly rotating stars they may become unstable if the viscous time scales are long enough. For a given mode, the angular velocity where the transition from stability to instability takes place is called the *critical* angular velocity  $\Omega_c$ . It is the root of the equation

$$0 \equiv \frac{1}{\tau(\Omega_c)} = \frac{1}{\tau_{\text{GR}}(\Omega_c)} + \frac{1}{\tau_\zeta(\Omega_c)} + \frac{1}{\tau_\eta(\Omega_c)}. \quad (37)$$

A given sequence of rotating stellar models is stable, then, only for angular velocities smaller than the smallest critical angular velocity  $\Omega_c$ .

The critical angular velocities of a sequence of rotating stellar models can be determined by finding the roots of equation (37). A more useful form of this equation may be obtained by using the functions that describe the angular-velocity dependence of the various dissipative time scales,  $\beta_m(\Omega)$ ,  $\gamma_m(\Omega)$ , and  $\epsilon_m(\Omega)$ , and the function  $\alpha_m(\Omega)$  (see Paper I) that describes the angular-velocity dependence of the frequency of the non-dissipative mode  $\omega_m$ :

$$\alpha_m(\Omega) = \frac{\omega_m(\Omega) + m\Omega}{\omega_m(0)}. \quad (38)$$

Thus, substituting equations (34), (35), (36), and (38) into equation (37) we obtain

$$\Omega_c = \frac{\omega_m(0)}{m} \left\{ \alpha_m(\Omega_c) + \gamma_m(\Omega_c) \left[ \frac{\tau_{\text{GR}}(0)}{\tau_\eta(0)} \right]^{1/(2l+1)} \times \left[ 1 + \frac{\tau_\eta(0)}{\tau_\zeta(0)} \frac{\epsilon_m(\Omega_c)}{1 - (\Omega_c/\Omega_{\text{max}})^4} \right]^{1/(2l+1)} \right\}. \quad (39)$$

This equation depends only on the dissipative time scales of nonrotating stellar models  $\tau_{\text{GR}}(0)$ ,  $\tau_\eta(0)$ , and  $\tau_\zeta(0)$  and the slowly varying and relatively equation of state independent functions  $\alpha_m(\Omega)$ ,  $\gamma_m(\Omega)$ , and  $\epsilon_m(\Omega)$ . In the case where the effects of bulk viscosity are negligible compared to shear viscosity,  $\tau_\zeta \gg \tau_\eta$ , this equation reduces to the one given by Lindblom (1986).

Equation (39) is easily solved numerically. The initial estimate  $\Omega_c \approx \omega_m(0)/m$  can be inserted into the right side of equation (39) with the result being a better estimate. A few iterations of this procedure produce an accurate value of  $\Omega_c$ . Figure 17 illustrates the results of such computations. Each curve represents the smallest critical angular velocity  $\Omega_c$  associated with the  $l = m$   $f$ -modes for a sequence of constant-mass stellar models based on the indicated equation of state. These critical angular velocities are given in units of  $\Omega_{\text{max}}$ , the maximum angular velocity that exists for equilibrium stellar models having that mass and equation of state. These “Keplerian” angular velocities depend on the equation of state, and have the values  $\Omega_{\text{max}} = 0.648\Omega_0$ ,  $0.639\Omega_0$ , and  $0.626\Omega_0$  for the  $n = 3/4, 1,$  and  $5/4$  polytropes, respectively. Since the viscous time scales  $\tau_\eta$  and  $\tau_\zeta$  depend on the temperature of the star, these critical angular velocities are temperature-dependent as well. The dashed curves represent critical angular velocities that neglect the effects of bulk viscosity. We see that in neutron stars cooler than  $T \approx 10^6 \sim 7$  K the shear viscosity is sufficiently

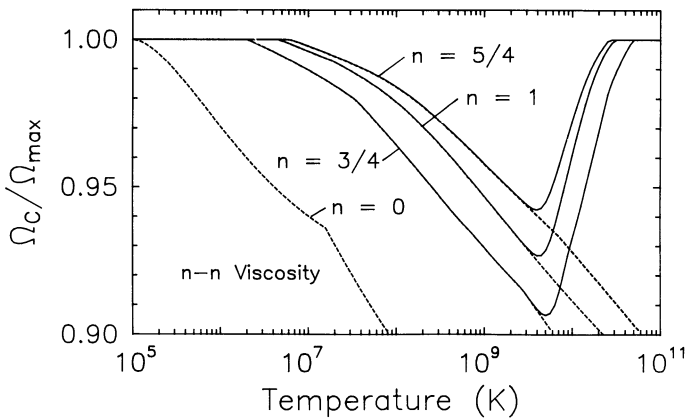


FIG. 17.—Critical angular velocities  $\Omega_c$  as functions of the temperature for  $1.5 M_\odot$  polytropes of indices  $n = 0, 3/4, 1,$  and  $5/4$ . The angular velocities are given in units of  $\Omega_{\max}$ , the maximum angular velocity for which an equilibrium stellar model exists of the same mass. The dashed curves ignore the effects of bulk viscosity.

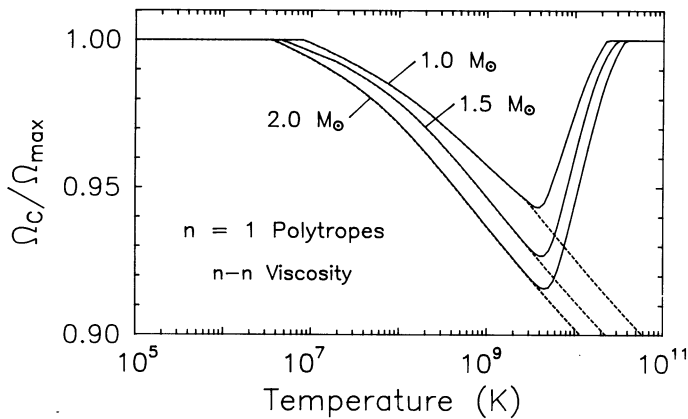


FIG. 18.—Critical angular velocities  $\Omega_c$  as functions of the temperature for  $1.0, 1.5,$  and  $2.0 M_\odot$  polytropes of index  $n = 1$ . The angular velocities are given in units of  $\Omega_{\max}$ , the maximum angular velocity for which an equilibrium stellar model exists of the same mass. The dashed curves ignore the effects of bulk viscosity.

large to completely suppress the gravitational-radiation driven instability. Similarly, in neutron stars hotter than  $T \approx 2 \times 10^{10}$  K the bulk viscosity is sufficiently large to suppress this instability. For intermediate temperatures the instability may occur, but only for stars rotating faster than 90%  $\sim$  95% of the speed at which mass would be ejected from the star by centrifugal forces. The curves in Figure 17 indicate that the angular velocities of stars based on stiffer equations of state are more strongly limited than those based on softer equations of state. Figure 18 compares the critical angular velocities of stars of different masses. The angular velocities of more massive stars are more strongly limited than those of less massive stars. This occurs because the destabilizing influence of gravitational radiation couples more strongly to more massive stars. Finally, Figure 19 illustrates the sensitivity of these critical angular velocities to the assumed form of the shear viscosity. The viscosity of neutron-star matter is not well

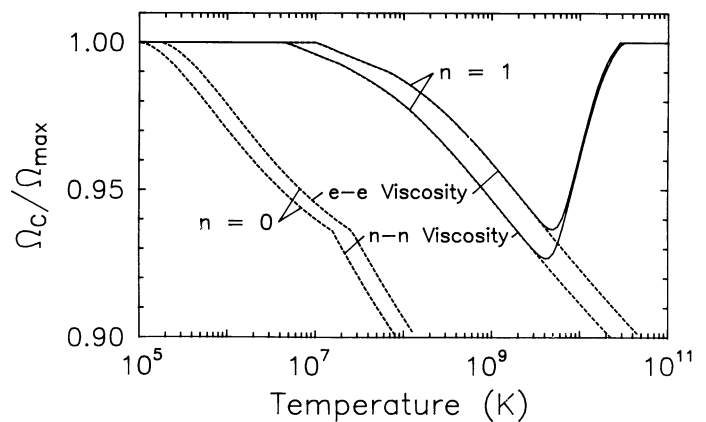


FIG. 19.—Critical angular velocities  $\Omega_c$  as functions of the temperature based on two different expressions for the shear viscosity: neutron-neutron scattering viscosity  $\eta_n$  and electron-electron scattering viscosity  $\eta_e$ . The angular velocities are given in units of  $\Omega_{\max}$ , the maximum angular velocity for which an equilibrium stellar model exists of the same mass. The dashed curves ignore the effects of bulk viscosity.

understood. These curves illustrate, however, that the critical angular velocities are rather insensitive to the form of the viscosity law. Furthermore, the temperature in the expression for the viscosity serves as an adjustable free parameter. An error of one order of magnitude in the viscosity law corresponds to shifting these critical angular velocity curves only by a factor of 3 along the temperature axis.

The estimates of the critical angular velocities of neutron stars presented in this paper are based on the self-consistent Newtonian computations of the modes of rotating stars developed in Paper I and extended here to include dissipative effects. Real neutron stars are, of course, governed by the laws of general relativistic hydrodynamics. The extent to which relativistic effects will modify these Newtonian estimates cannot be known with certainty until the far more difficult fully relativistic calculation of the modes of these stars is completed. We anticipate, however, that the relativistic corrections to the estimates of the critical angular velocities will be small, when presented in the form given here. In particular we expect that the critical angular velocities will be approximately 90%–95% of the *relativistic* Keplerian angular velocities. This expectation is based on earlier computations of the critical angular velocities based on relativistic values of  $\omega(0)$ ,  $\tau_{\text{GR}}(0)$  and  $\tau_\eta(0)$  but using the Maclaurin spheroid functions  $\alpha_m(\Omega)$  and  $\tau_m(\Omega)$  (Lindblom 1986, 1987, 1988). Those results do not differ substantially from the ones presented here. Further, a post-Newtonian computation of the functions  $\alpha_m(\Omega)$  by Cutler & Lindblom (1991, in preparation) indicates that these functions differ from their Newtonian counterparts by only a few percent at the critical angular velocities.

This research was supported by grants PHY-8518490, PHY-8906915, and PHY-9019753 from the National Science Foundation. L. L. thanks the Institute for Fundamental Theory of the University of Florida for their hospitality during several visits during which portions of this work were completed.



## REFERENCES

- Cutler, C., & Lindblom, L. 1987, ApJ, 314, 234  
Cutler, C., Lindblom, L., & Splinter, R. J. 1990, ApJ, 363, 603  
Flowers, E., & Itoh, N. 1976, ApJ, 206, 218  
Friedman, J. L. 1983, Phys. Rev. Letters, 51, 11  
Ipser, J. R., & Lindblom, L. 1989, Phys. Rev. Letters, 62, 2777; erratum 63, 1327  
———. 1990, ApJ, 355, 226 (Paper I)  
Landau, L. D., & Lifshitz, E. M. 1975, Fluid Mechanics (Oxford: Pergamon Press)
- Lindblom, L. 1986, ApJ, 303, 146  
———. 1987, ApJ, 317, 325  
———. 1988, in Experimental Gravitational Physics, ed. P. F. Michelson (Singapore: World Scientific), p. 276  
Sawyer, R. F. 1989, Phys. Rev. D, 39, 3804  
Thorne, K. S. 1969, ApJ, 158, 997  
Wagoner, R. V. 1984, ApJ, 278, 345